New Insights into Water Treatment Materials with Chemically Sensitive Soft and Tender X-rays

Gregory M. Su,[a,b,*] Isvar A. Cordova,[b] and Cheng Wang[a]

[a]*Advanced Light Source, Lawrence Berkeley National Laboratory, Berkeley, CA 94720 USA;* [b]*Materials Sciences Division, Lawrence Berkeley National Laboratory, Berkeley, CA 94720 USA*

*email: gsu@lbl.gov

New Insights into Water Treatment Materials with Chemically Sensitive Soft and Tender X-rays

Keywords: resonant x-ray scattering; x-ray absorption spectroscopy; soft x-ray; tender x-ray; water treatment; membrane; polymer; morphology

Subject classification codes: include these here if the journal requires them

Introduction

Adequate access to clean, safe water is required for humanity's well-being and continued prosperity. However, over one billion people around the world lack this access [1,2]. Materials science and nanotechnology advancements are needed to solve this global challenge [3,4]. Polymer materials play a critical role in water treatment processes ranging from coagulants for impurity removal [5,6] to membranes for filtration and reverse osmosis (RO) [7]. However, polymer-based materials design still largely relies on an Edisonian approach. Improved fundamental knowledge connecting polymer chemistry, structure and morphology, and performance is needed for molecular-level, fit-for-purpose design to target specific water treatment needs [3,8]. Membrane-based RO is the most energy-efficient desalination process [9]. However, challenges remain, for example, membranes suffer from fouling [10] and are poor at rejecting certain species, such as boron [11].

Polymers are often relatively disordered and there is limited elemental contrast among its constituent elements. This drives the need for unique tools that can probe molecular assembly and morphology combined with chemical sensitivity in these complex systems. Energy-tunable synchrotron X-rays in the soft (~100 eV-2000 eV) and tender (~2,000 eV-8,000 eV) energy regimes span the absorption edges of the most common elements found in polymers, including C, N, O, and S, enabling unique elemental and functional group sensitivity. Moreover, many of the most common

elements found in seawater (e.g. Na and Cl) and the elements involved in membrane fouling from inorganic substances, or scaling (e.g. Ca and Si) have core-level absorption edges within the soft and/or tender X-ray regimes. This presents opportunities for energy-resolved synchrotron X-ray characterization to provide new insights into, among other aspects, the morphology of polymers for water treatment and the interactions of polymers with water and dissolved species.

In this contribution, we highlight some of the unique opportunities chemically sensitive energy-tunable synchrotron X-ray characterization provides for detailed understanding of polymers for water treatment. We focus on polymer-based membranes that are widely used for desalination and filtration. Although an array of synchrotron methods can play an important role in advancing water treatment materials, we highlight the potential of energy-tunable X-ray scattering coupled with near edge X-ray absorption fine structure (NEXAFS) spectroscopy to probe membrane structure and chemistry. The terminology resonant soft X-ray scattering (RSoXS) and tender resonant X-ray (TReXS) has been used in the literature to specify the X-ray energy range, but for simplicity, we will refer to this generally as resonant X-ray scattering (RXS). RXS of soft materials is an emerging capability that has seen limited use for water treatment membranes. We will briefly highlight recent studies that leverage RXS to decipher water treatment membrane structure and showcase opportunities for *in situ* experiments that span the soft and tender regimes coupled with simulations to address challenges going forward.

Chemically resolving nano- to mesoscale morphology

Morphology defines the performance of water treatment membranes. For example, the crosslink density and free volume in a RO membrane or the pore size and size distribution in a filtration membrane dictate transport and selectivity. Understanding and

controlling membrane morphology based on polymer chemistry and processing conditions is required for next-generation materials. Important insights into the morphology of water treatment membranes have been achieved through characterization tools, including electron microscopy [12–14], neutron scattering [15–17], and hard X-ray scattering [18,19].

X-ray and neutron scattering can non-destructively probe soft matter morphology spanning sub-nanometer to hundreds of nanometers in scale. However, the low scattering cross-section of polymer membranes, especially thin films, limits the capability of hard X-rays and neutrons to gain sufficient quantitative information. Chemical labelling techniques, e.g., the substitution of hydrogen with deuterium used in neutron scattering, are therefore required for contrast matching and enhancement. The recent development of soft RXS at the Advanced Light Source (ALS) [20] provides a unique complementary approach to study soft materials. Combining conventional X-ray scattering with soft X-ray NEXAFS, soft RXS is a unique chemically sensitive structural probe that provides a novel route to unambiguously decipher the complex morphologies of mesoscale materials. RXS can selectively enhance the scattering contribution from different chemical components by tuning the X-ray energy to match the absorption spectrum of the respective component [21], enabling a glimpse into these complex morphologies with unprecedented detail.

RXS can distinctly probe the unique phases in a multicomponent porous polymer membrane. Contrast-matched RXS studies on the morphology of a mesoporous polystyrene-*b*-polyethylene-*b*-polystyrene (SES) block copolymer membrane with pores lined by the polystyrene (PS) phase uniquely revealed the microphase separation between polystyrene and polyethylene, as shown in Figure 1a [22]. Conventional techniques such as hard X-ray small-angle X-ray scattering (SAXS) and scanning

electron microscopy (SEM) can only distinguish between the polymer and the voids. In a follow-on study, the SES copolymer was mixed with PS homopolymer and rinsed with either tetrahydrofuran or methanol to create a porous structure. The PS phase was sulfonated to create hydrophilic domains. The membrane porosity was found to impact the water uptake and ion transport in these block copolymer membranes [23].

Soft X-ray RXS provides critical insights into the structure of dense, amorphous thin polyamide films that are the industry standard for RO membranes and particularly challenging to characterize. A recent study looked at commercial polyamide membranes synthesized using interfacial polymerization with varying degrees of crosslink density. Transmission soft RXS was able to decouple internal membrane chemical heterogeneities from roughness effects by a judicious choice of incident X-ray energy and correlate this internal structure to crosslink density (Figure 1b-c) [24]. A complementary study investigated model, smooth polyamide thin films formed by a layer-by-layer method and quantified functional group concentration as a function of depth using resonant soft X-ray reflectivity. Functional group concentration impacts the membrane's permselectivity, and it was found that more densely crosslinked membranes have a higher permselectivity [25]. These initial water treatment membrane studies using RXS clearly show the important role energy-tunable synchrotron X-rays will play in advancing membrane technology.

Emerging opportunities to probe membrane interactions and structure in realistic environments

In situ synchrotron X-ray studies

Designing next-generation water treatment membranes requires understanding membrane behavior in realistic environments. Synchrotron X-ray scattering and

spectroscopy are well-suited to probe *in situ* membrane-solute interactions and membrane morphology. *In situ* RXS coupled with NEXAFS is promising for selectively deciphering local interactions among organic and inorganic species and the distribution of distinct domains in a phase-separated membrane, e.g., the selective swelling or adsorption of solutes in a hydrophilic domain lining inner pore walls.

Experiments at different X-ray energy ranges require unique environments. The high vacuum chambers needed for soft X-ray measurements presents a practical challenge for *in situ* studies with water. Vacuum-compatible liquid flow cells developed for *in situ* transmission electron microscopy (TEM) can be adapted for soft X-ray measurements including scattering, spectroscopy, and transmission microscopy [26,27]. Ion conducting polymers, or ionomers, are important for electrochemical energy conversion applications and water treatment membranes that selectively reject certain charged species. Perfluorinated ionomers are commonly used as ion exchange membranes. They exhibit a nanoscale phase separated morphology that forms hydrophilic ion transport pathways [28]. Phase-separated ionomer thin films typically show two main scattering features. One is representative of the average distance between semicrystalline hydrophobic domains and the other, typically at smaller length scales, reflects the average spacing between hydrophilic, or ionomer, domains. The ionomer domains are known to swell under hydrated conditions [28]. However, these thin films' scattering signals can be particularly difficult to resolve under *in situ* conditions due to attenuation effects from the surrounding water volume, but scattering contrast can be significantly enhanced at energies near an appropriate elemental absorption edge. Figure 2 shows *in situ* transmission RXS of ionomer thin films submerged in water at energies near the absorption K-edges of constituent elements, in this case O and F. Changes in the incident X-ray beam's energy of a few eV noticeably

affect scattering contrast and serve to amplify the semicrystalline domain peak. These measurements were taken in the high vacuum scattering chamber at beamline 11.0.1.2 at the ALS [20] using an *in situ* cell specifically modified for the beamline developed in collaboration with Protochips, a manufacturer of commercial *in situ* TEM equipment. The phase-separated ionomer thin film membrane shows a scattering feature representative of the average domain spacing, and this domain spacing changes under hydrated conditions. Furthermore, the scattering signal is enhanced at energies near the absorption edges of constituent elements, such as the O and F K-edges shown in Figure 2.

Transmission RXS of semicrystalline polymers can show anisotropic scattering patterns, and this is thought to arise from the local orientation of polymer chains and the sensitivity of polarized X-rays to the direction of core-level transition dipole moments. Polarized RXS provides a unique probe of polymer chain orientation, or even specific functional groups, allowing RXS to decipher structural details such as chain alignment at domain interfaces. This has been demonstrated for conjugated polymers [29,30], and continued development in quantitative analysis of polarized scattering will enable new insights into multicomponent water treatment membranes, e.g., the orientation of polymer chains lining the pores of an isoporous membrane or the adsorption configuration of molecules within those pores. Overall, this demonstrates the utility of *in situ* RXS to probe polymer membrane morphology, especially for thin films. Soft X-ray scattering is well-suited to probing the in-plane mesoscale structure of thin polymer films under realistic environments relevant for water treatment, providing opportunities to study the morphology of the thin, dense rejection layer of a thin film composite (TFC) RO membrane, porous membranes, and other systems.

Future next-generation membranes will need to go beyond separating species based on size and rely on precise functionalization to be stimuli responsive, charge-selective, or even separate species of similar charge [8,31]. Progress in polymer synthesis, membrane functionalization, and self-assembly has enabled membranes that exhibit tailored functionalities. For example, a triblock terpolymer based on poly(styrene)-*b*-poly(4-vinylpyridine)-*b*-poly(propylene sulfide) forms a porous ultrafiltration membrane with sulfhydryl functional groups serving as covalent binding sites within the pores. These sites can interact with specific molecules through thiol-ene click chemistry [32]. Another recent study demonstrated that a nanoporous membrane formed from an amphiphilic triblock terpolymer, P(HTMB-*r*-I)-*b*-PS-*b*-P4VP, contains -OH and 4VP functional groups that can be treated through a gas-solid reaction to form inner pore walls decorated with positively or negatively charged moieties. These membranes exhibit good selectivity of small organic molecules (1-2 nm in size) based on size and charge [33].

These chemical interactions will need to be interrogated under *in situ* conditions to inform the design of fit-for-purpose membranes. Element-specific XAS provides sensitivity to specific chemical bonds and functional groups. When guided by first-principles predictions [34,35], XAS can characterize specific molecular interactions. This renders theory-guided XAS a promising tool to unravel membrane-solute interactions *in situ* that define performance. Coupled with the spatial sensitivity of RXS, new opportunities exist for comparing the molecular interactions among distinct domains in a phase-separated membrane.

Leveraging tender X-rays

Tender X-rays offer new opportunities for detailed characterization of water treatment materials with sensitivity to important elements involved in membrane processes. With

the growing number of tender X-ray resonant scattering and spectroscopy beamlines, these techniques are poised to impact water treatment research.

Although there are only few reports of tender RXS on polymer materials, recent studies showcase its utility to enhance scattering contrast and elucidate membrane morphology with chemical sensitivity, specifically on perfluorinated ionomers [36,37]. Ionomers are widely used for electrochemical energy conversion applications such as fuel cells, and their ion-conducting properties are translatable to water treatment. For example, a photoacid-modified perfluorinated ionomer was recently shown to have light-driven ionic activity, promising for solar-driven desalination [38,39]. The impact of chemical modification on membrane morphology is challenging to predict. As shown in Figure 3a, tender RXS performed at ALS beamline 5.3.1 reveals that the characteristic domain spacing increases with increasing amount of attached photoacid dye [37], providing new insights into the structure of membranes for solar-driven desalination.

Figure 3b shows tender RXS curves at 2476 eV for a library of ionomers with varying side-chain lengths and number of sulfur-containing acidic groups. RXS at the S K-edge reveals membranes with nanoscale phase separation and a systematic increase in average domain spacing with polymer side-chain length. Furthermore, *in situ* RXS reveals the increase in domain spacing upon hydration. Beyond membrane nanoscale morphology, S K-edge NEXAFS has the potential to determine hydration state and local hydrogen bonding configuration, and this is demonstrated through first-principles NEXAFS predictions based on density functional theory (DFT), as shown in Figure 4.

Sensitivity to elements, including S, Cl, and Ca, enables tender X-ray scattering and spectroscopy to probe the diffusion, distribution, and deposition of species relevant to desalination and inorganic fouling. Fouling remains one of the main causes of

reduced permeate flux in membranes and an ongoing challenge to solve. In addition to fouling by organic species, the build-up of inorganic foulants, also known as scaling, occurs due to precipitation of ions from the feed water. Calcium sulfate, $CaSO_4$, and calcium carbonate, $CaCO_3$, scales are among the major causes of fouling in membranes. Scale deposition not only hinders membrane performance, but also promotes organic fouling. RO and other membranes with anti-scaling properties are being investigated to develop more environmentally friendly membranes that can resist performance losses [40]. Tender X-rays span the absorption K-edge of Ca, which is near 4.0 keV, presenting an opportunity for X-ray techniques in this energy range to characterize the build-up of Ca-based scales both on the membrane surface and within membrane pores. Judicious energy tuning could distinguish between different Ca-containing species, e.g., $CaCO_3$ and $CaSO_4$.

Probing dynamic membrane processes

Membranes are often formed via dynamic processes and can undergo structural changes in response to unique water environments. Understanding and controlling time-dependent membrane evolution is an important step towards molecular-level design, and synchrotron tools have proven critical and will continue to advance this field.

Block copolymer self-assembly is a scalable, industrially relevant route to produce isoporous membranes. The nano- to mesoscale molecular assembly in membranes must be understood in the context of large-scale processing methods. Previous work has employed hard X-ray small angle scattering to track the *in situ* morphology evolution of solution-cast block copolymer membranes [41–44] (**Figure *5***a) and other functional polymers [45]. Non-solvent induced phase separation in combination with block copolymer self-assembly produces integral asymmetric membranes (IAMs) that have a selective, nanoporous thin layer atop a more porous, less

ordered sponge-like layer [46]. One study found that a structural feature in the range of 30-70 nm (dependent on the molecular weight of the block copolymer) appears within the first 20 s after solvent casting. This feature increases in length-scale with time, reaching a plateau by 100 s (Figure 5b). Interestingly, immersion in water causes the characteristic length-scale measured by scattering to quickly transition to the plateau value [44]. A separate study utilized grazing incidence small-angle X-ray scattering to show the surface morphology of an asymmetric triblock terpolymer transitions from a disordered state, to a body-cantered cubic to a simple cubic morphology [42]. Going beyond hard X-rays, tracking membrane morphology development during fabrication using *in situ* RXS will enable increased contrast and opportunities to leverage energy-resolved contrast matching to selectively track the evolution of selective phases, e.g., domains lining the inner pore walls. The high vacuum chambers needed for soft RXS make studying evaporation-induced morphology evolution challenging. However, the vacuum-compatible flow cells discussed earlier and shown in Figure 2 should be leveraged to advance these studies. The multiple microfluidic lines in these flow cells would allow for experiments that involve exposing a thin film polymer membrane to a solvent to induce assembly followed by introduction of a non-solvent or dry nitrogen gas to mimic non-solvent or evaporation-induced assembly. *In situ* X-ray characterization is also promising for tracking foulant build-up on membranes. The chemical sensitivity of RXS would likely allow new insights into the independent formation rates of external versus internal fouling.

Coherent X-ray scattering methods, including X-ray photon correlation spectroscopy (XPCS) are capable of probing polymer chain dynamics and diffusion in nanostructured systems like block copolymers [35,47]. Future synchrotron upgrades to diffraction-limited storage rings will greatly enhance XPCS capabilities. Specifically,

resonant XPCS using soft or tender X-rays will be advanced at upgraded synchrotrons, for example, ALS-U. Resonant XPCS that leverages the chemical sensitivity of energy-tunable X-rays has yet to be applied to polymers and membranes and has the opportunity to transform capabilities to measure not only the motion of polymer chains, but also the diffusion of solutes and compounds that penetrate water treatment membranes.

Conclusion

Addressing the water-energy nexus and water treatment is a global challenge. Technological advancement will rely on the development of new membrane materials with tailored properties through an understanding of how molecular design impacts molecular interactions and assembly across length-scales. Synchrotron-based resonant X-ray scattering and X-ray absorption spectroscopy coupled with theory are poised to provide new insights into polymer membrane morphology with chemical sensitivity under realistic environments, and these capabilities will advance with next-generation lightsource upgrades. This unique suite of tools should continue to grow to be an integral part of the water treatment communities seeking to advance polymer and membrane materials.

Acknowledgements

The authors thank Ahmet Kusoglu and Peter Dudenas for providing ion-conducting membranes showcased in this work.

Funding

This work was supported by the Advanced Light Source (ALS) user facility located at the Lawrence Berkeley National Laboratory and supported by the Director, Office of

Science, Office of Basic Energy Sciences, of the U.S. Department of Energy under Contract No. DE-AC02-05CH11231.

References:

[1] M.A. Shannon, P.W. Bohn, M. Elimelech, J.G. Georgiadis, B.J. Marĩas and A.M. Mayes, *Nature* **452**(7185), 301–310 (2008).

[2] *World Econ. Forum Glob. Risks Rep.* , 1–114 (2020).

[3] J.R. Werber, C.O. Osuji and M. Elimelech, *Nat. Rev. Mater.* **1** (2016).

[4] M.S. Mauter, I. Zucker, F. Perreault, J.R. Werber, J.H. Kim and M. Elimelech, *Nat. Sustain.* **1**(4), 166–175 (2018).

[5] B. Bolto and J. Gregory, *Water Res.* **41**(11), 2301–2324 (2007).

[6] M. Nadella, R. Sharma and S. Chellam, *Water Res.* **170**, 115330 (2020).

[7] G.M. Geise, H.-S. Lee, D.J. Miller, B.D. Freeman, J.E. McGrath and D.R. Paul, *J. Polym. Sci. Part B Polym. Phys.* **48**(15), 1685–1718 (2010).

[8] Y. Zhang, N.E. Almodovar-Arbelo, J.L. Weidman, D.S. Corti, B.W. Boudouris and W.A. Phillip, *npj Clean Water* **1**(1), 1–14 (2018).

[9] L.F. Greenlee, D.F. Lawler, D. Freeman, Benny, M. Benoit and P. Moulin, *Water Res.* **43**(9), 2317–2348 (2009).

[10] D.J. Miller, D.R. Dreyer, C.W. Bielawski, D.R. Paul and B.D. Freeman, *Angew. Chemie - Int. Ed.* **56**(17), 4662–4711 (2017).

[11] J. Wolska and M. Bryjak, *Desalination* **310**(214), 18–24 (2013).

[12] T.E. Culp, Y.X. Shen, M. Geitner, M. Paul, A. Roy, M.J. Behr et al., *Proc. Natl. Acad. Sci. U. S. A.* **115**(35), 8694–8699 (2018).

[13] X. Song, J.W. Smith, J. Kim, N.J. Zaluzec, W. Chen, H. An et al., *ACS Appl. Mater. Interfaces* **11**(8), 8517–8526 (2019).

[14] X. Song, B. Gan, S. Qi, H. Guo, C.Y. Tang, Y. Zhou et al., *Environ. Sci. Technol.* **54**(6), 3559–3569 (2020).

[15] F. Foglia, S. Karan, M. Nania, Z. Jiang, A.E. Porter, R. Barker et al., *Adv. Funct. Mater.* **27**(37), 18–20 (2017).

[16] E.P. Chan, B.R. Frieberg, K. Ito, J. Tarver, M. Tyagi, W. Zhang et al., *Macromolecules* **53**(4), 1443–1450 (2020).

[17] T. Kawakami, M. Nakada, H. Shimura, K. Okada and M. Kimura, *Polym. J.* **50**(4), 327–336 (2018).

[18] Q. Fu, N. Verma, H. Ma, F.J. Medellin-Rodriguez, R. Li, M. Fukuto et al., *ACS Macro Lett.* **8**(4), 352–356 (2019).

[19] X. Lu, X. Feng, Y. Yang, J. Jiang, W. Cheng, C. Liu et al., *Nat. Commun.* **10**(1), 3–9 (2019).

[20] E. Gann, A.T. Young, B.A. Collins, H. Yan, J. Nasiatka, H.A. Padmore et al., *Rev. Sci. Instrum.* **83**(4) (2012).

[21] C. Wang, D.H. Lee, A. Hexemer, M.I. Kim, W. Zhao, H. Hasegawa et al., *Nano Lett.* **11**(9), 3906–3911 (2011).

[22] D.T. Wong, C. Wang, K.M. Beers, J.B. Kortright and N.P. Balsara, *Macromolecules* **45**(22), 9188–9195 (2012).

[23] X.C. Chen, J.B. Kortright and N.P. Balsara, *Macromolecules* **48**(16), 5648–5655 (2015).

[24] T.E. Culp, D. Ye, M. Paul, A. Roy, M.J. Behr, S. Jons et al., *ACS Macro Lett.* **7**(8), 927–932 (2018).

[25] D.F. Sunday, E.P. Chan, S. V Orski, R.C. Nieuwendaal and C.M. Stafford, *Phys. Rev. Mater.* **2**(3), 32601 (2018).

[26] Y. Li, J.N. Weker, W.E. Gent, D.N. Mueller, J. Lim, D.A. Cogswell et al., *Adv. Funct. Mater.* **25**(24), 3677–3687 (2015).

[27] J. Lim, Y. Li, D.H. Alsem, H. So, S.C. Lee, P. Bai et al., *Science* **353**(6299), 566–571 (2016).

[28] A. Kusoglu and A.Z. Weber, *Chem. Rev.* **117**(3), 987–1104 (2017).

[29] B.A. Collins, J.E. Cochran, H. Yan, E. Gann, C. Hub, R. Fink et al., *Nat. Mater.* **11**(6), 536–43 (2012).

[30] J.H. Litofsky, Y. Lee, M.P. Aplan, B. Kuei, A. Hexemer, C. Wang et al., *Macromolecules* **52**(7), 2803–2813 (2019).

[31] M. Radjabian and V. Abetz, *Prog. Polym. Sci.* **102**, 101219 (2020).

[32] Q. Zhang, Y. Gu, Y.M. Li, P.A. Beaucage, T. Kao and U. Wiesner, *Chem. Mater.* **28**, 3870–3876 (2016).

[33] Z. Zhang, M. Rahman, C. Abetz and A. Höhme, *Adv. Mater.* **32**, 1907014 (2020).

[34] G.M. Su, S.N. Patel, C.D. Pemmaraju, D. Prendergast and M.L. Chabinyc, *J. Phys. Chem. C* **121**(17), 9142–9152 (2017).

[35] G.M. Su, I.A. Cordova, M.A. Brady, D. Prendergast and C. Wang, *Polymer* **105**(22), 342–356 (2016).

[36] G.M. Su, I.A. Cordova, M.A. Yandrasits, M. Lindell, J. Feng, C. Wang et al., *J. Am. Chem. Soc.* **141**(34), 13547–13561 (2019).

[37] G.M. Su, W. White, L.A. Renna, J. Feng, S. Ardo and C. Wang, *ACS Macro Lett.* **8**(10), 1353–1359 (2019).

[38] W. White, D. Christopher, D.M. Fabian, W. White, C.D. Sanborn, D.M. Fabian et al., *Joule* **2**, 1–16 (2018).

[39] W. White, C.D. Sanborn, R.S. Reiter, D.M. Fabian and S. Ardo, *J. Am. Chem. Soc.* **139**(34), 11726–11733 (2017).

[40] Y. Takizawa, S. Inukai, T. Araki, R. Cruz-silva, J. Ortiz-medina, A. Morelos-gomez et al., *ACS Omega* **3**, 6047–6055 (2018).

[41] C. Stegelmeier, V. Filiz, V. Abetz, J. Perlich, A. Fery, P. Ruckdeschel et al., *Macromolecules* **47**(16), 5566–5577 (2014).

[42] Y. Gu, R.M. Dorin, K.W. Tan, D.M. Smilgies and U. Wiesner, *Macromolecules* **49**(11), 4195–4201 (2016).

[43] K. Sankhala, D.C.F. Wieland, J. Koll, M. Radjabian, C. Abetz and V. Abetz, *Nanoscale* **11**(16), 7634–7647 (2019).

[44] C. Stegelmeier, A. Exner, S. Hauschild, V. Filiz, J. Perlich, S. V. Roth et al., *Macromolecules* **48**(5), 1524–1530 (2015).

[45] F. Liu, S. Ferdous, E. Schaible, A. Hexemer, M. Church, X. Ding et al., *Adv. Mater.* **27**, 886–891 (2015).

[46] K. Peinemann, V. Abetz and P.F.W. Simon, **6**(December) (2007).

[47] O. Oparaji, S. Narayanan, A. Sandy, S. Ramakrishnan and D. Hallinan, *Macromolecules* **51**(7), 2591–2603 (2018).

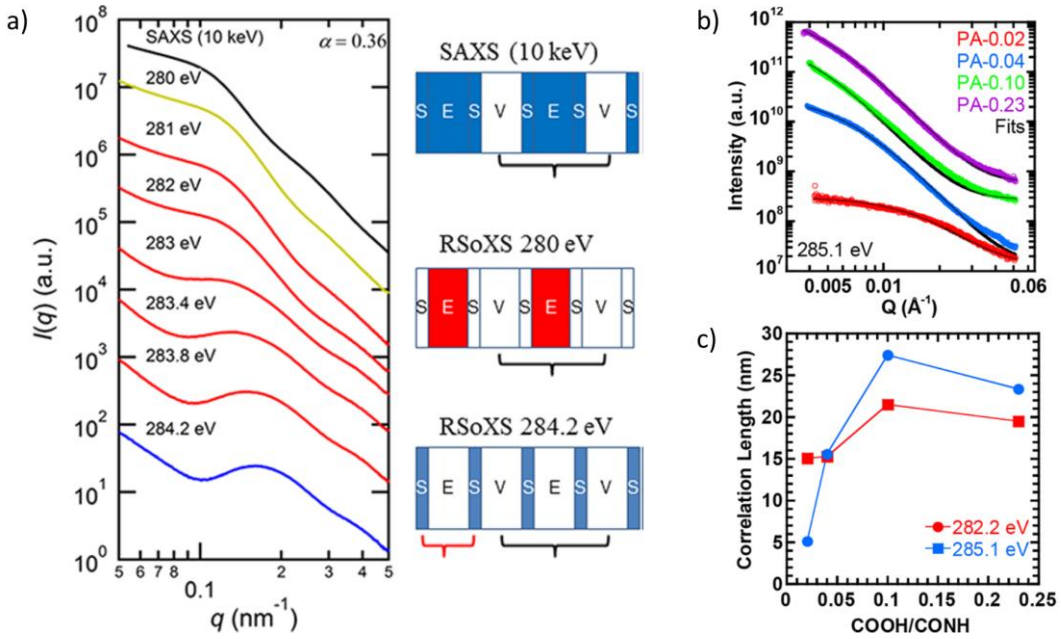

Figure 1. RXS profiles of a mesoporous block copolymer, with schematics of the microphase separation probed at representative energies, are shown in (a). The specific polymer domains and unique morphological features are probed depending on the incident X-ray energy, allowing for precisely distinguishing the distance between voids and the distance between polystyrene domains. Reprinted with permission from Ref. [22]. Copyright 2012 American Chemical Society. RXS at 285.1 eV for commercially made polyamide RO membranes with varying acid to amide ratio is shown in (b). The correlation length of the internal membrane heterogeneities as a function of the acid to amide ratio is shown in (c). Reprinted with permission from Ref. [24]. Copyright 2018 American Chemical Society.

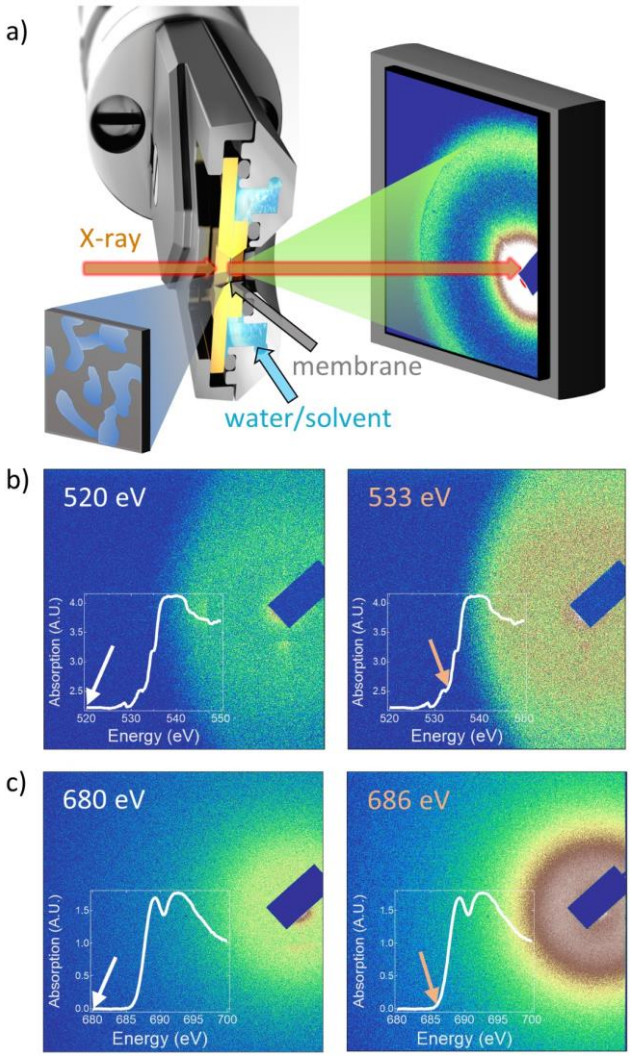

Figure 2. (a) A cross-sectional schematic depicting the tip of a vacuum-compatible *in situ* TEM cell that has been customized for transmission RXS measurements is shown in (a). The cell encapsulates a membrane sample between two silicon nitride windows and allows liquid to flow under atmospheric pressures. Examples of raw scattering data collected from ~400 nm thick Nafion ionomer films submerged in de-ionized water is shown in (b) and (c) with pre-edge energies (left) and energies near the absorption edge (right). Data shown in (b) is near oxygen K-edge energies and data presented in (c) is near fluorine K-edge energies. The plotted insets show the corresponding *in situ* transmission NEXAFS spectra for reference.

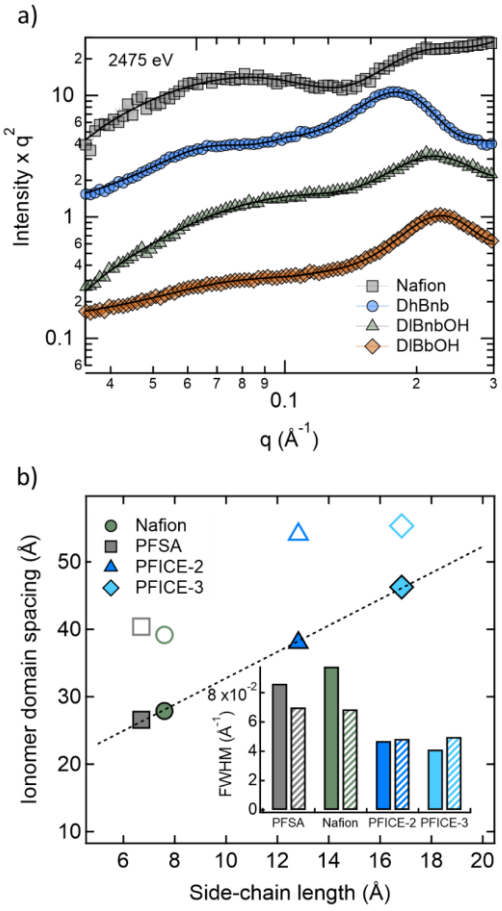

Figure 3. Transmission RXS data near the S K-edge (2475 eV) for photoacid-modified Nafion membranes is shown in (a). These measurements were collected at beamline 5.3.1 at the ALS. The dye content in the membranes trends as DhBnb > DlBnbOH > DlBbOH. Reprinted with permission from Ref. [37]. Copyright 2019 American Chemical Society. The hydrophilic ionomer domain spacing determined from RXS measurements at 2476 eV is shown in (b) for a series of perfluorinated ionomers with varying side-chain lengths. Filled symbols represent membranes under dry (ambient) conditions and the open symbols represent *in situ* measurements of membranes submerged in water. Reprinted with permission from Ref. [36]. Copyright 2019 American Chemical Society.

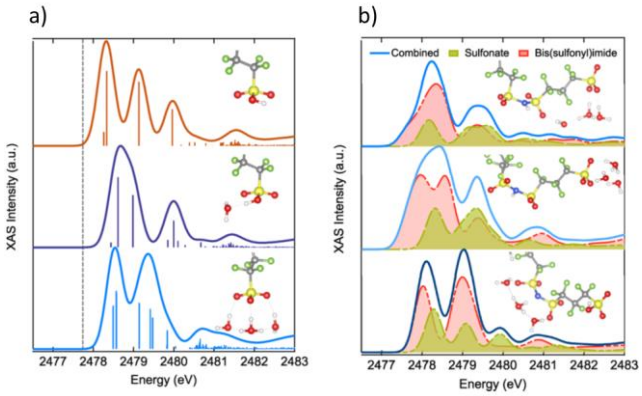

Figure 4. Simulated S K-edge NEXAFS data reveals the effects of (a) degree of hydration around the sulfonic acid group on an ionomer side-chain and (b) the hydrogen bonding configuration of three water molecules around an ionomer side-chain consisting of a sulfonic acid and a bis(sulfonyl)imide group. The corresponding structures are shown in the insets. Reprinted with permission from Ref. [36]. Copyright 2019 American Chemical Society.

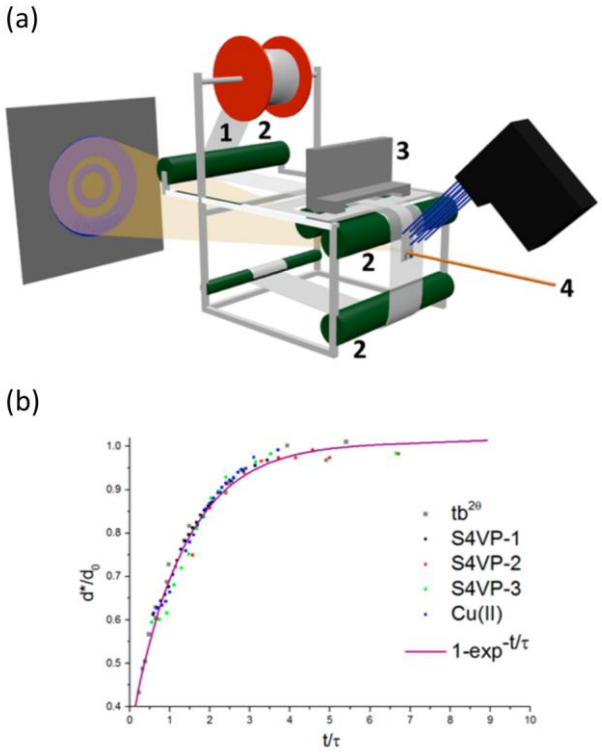

Figure 5. A schematic showing the film-casting setup used for *in situ* small angle X-ray scattering studies of evaporation-induced self-assembly of a block copolymer membrane is shown in (a). The characteristic membrane length scale during evaporation rescaled to a reduced time and reduce length-scale is plotted in (b) and shows similar

morphology evolution for a range of block copolymers. Reprinted with permission from Ref. [44]. Copyright 2015 American Chemical Society.